Tunable Reaction Potentials in Open Framework Nanoparticle Battery Electrodes for Grid-Scale Energy Storage

Colin D. Wessells,[†] Matthew T. McDowell,[†] Sandeep V. Peddada,[†] Mauro Pasta,[†] Robert A. Huggins,[†] and Yi Cui[†,‡,*]

[†]Department of Materials Science and Engineering, Stanford University, Stanford, California, 94305, United States, and [‡]Stanford Institute for Materials & Energy Science, SLAC National Accelerator Laboratory, 2575 Sand Hill Road, Menlo Park, California 94025, United States

ABSTRACT The electrical energy grid has a growing need for energy storage to address short-term transients, frequency regulation, and load leveling. Though electrochemical energy storage devices such as batteries offer an attractive solution, current commercial battery technology cannot provide adequate power, and cycle life, and energy efficiency at a sufficiently low cost. Copper hexacyanoferrate and nickel hexacyanoferrate, two open framework materials with the Prussian Blue structure, were recently shown to offer ultralong cycle life and high-rate performance when operated as battery electrodes in safe, inexpensive aqueous sodium ion and potassium ion electrolytes. In this report, we demonstrate that the reaction potential of copper–nickel alloy hexacyanoferrate nanoparticles may be tuned by controlling the ratio of copper to nickel in these materials. X-ray diffraction, TEM energy dispersive X-ray spectroscopy, and galvanostatic electrochemical cycling of copper–nickel hexacyanoferrate reveal that copper and nickel form a fully miscible solution at particular sites in the framework without perturbing the structure. This allows copper–nickel hexacyanoferrate to reversibly intercalate sodium and potassium ions for over 2000 cycles with capacity retentions of 100% and 91%, respectively. The ability to precisely tune the reaction potential of copper–nickel hexacyanoferrate without sacrificing cycle life will allow the development of full cells that utilize the entire electrochemical stability window of aqueous sodium and potassium ion electrolytes.

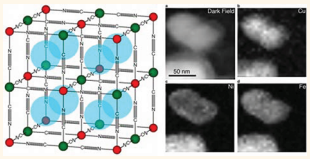

KEYWORDS: energy storage · batteries · nickel hexacyanoferrate · copper hexacyanoferrate · Prussian Blue · electric grid

The need for large-scale energy storage on the electrical power grid is growing rapidly. Energy storage capacity is already needed for frequency regulation and the management of short-term transients, which have proved to be extremely costly in recent years.[1,2] Widespread use of variable energy sources, such as solar and wind, will require immense energy storage capacity for load balancing. Pumped hydropower and compressed air are currently used for energy storage on the grid, but they require a high capital investment, have a low energy efficiency, and their use is location-dependent. Flywheel facilities offer high energy efficiency and power, but may not provide high enough energy to act as the primary energy storage source for the grid. Electrochemical energy storage devices such as batteries are desirable for use on a grid-wide scale, as they offer rapid response, high energy efficiency, and high energy density.[1–4]

Despite a growing need for energy storage devices on the electrical grid, both the research community and battery manufacturers have focused their efforts on the development of batteries for portable electronics and vehicles. As a result, most of the well-characterized materials systems used in batteries are not suitable for large-scale use on the electrical grid.[3,4] Lithium ion batteries provide insufficient cycle life at too high a cost to be used on large scales. The low cost of traditional lead acid batteries has made them more attractive for use on the grid, but they have low energy efficiency and suffer from poor cycle life even during shallow-discharge cycling. Redox flow batteries and high-temperature sodium/sulfur and sodium/nickel chloride batteries cannot be cycled quickly, and therefore can be used only for low power applications. In some cases, initial studies of aqueous lithium and sodium ion cells have shown good cycle life, but further development of the electrodes in these cells is needed.[5–7] In general, existing battery systems do not offer the ultralong cycle life, high power, and low cost needed for widespread use on the grid.

We recently showed that two promising new open framework battery electrode

* Address correspondence to yicui@stanford.edu.

Received for review December 1, 2011 and accepted January 29, 2012.

Published online January 29, 2012
10.1021/nn204666v

materials, copper hexacyanoferrate (CuHCF) and nickel hexacyanoferrate (NiHCF) offer long cycle life, high capacity retention during fast cycling, and very low hysteresis that allows development of devices with very high energy efficiency.[8−10] Bulk quantities of highly crystalline nanoparticles of these CuHCF and NiHCF were synthesized at or near room temperature from earth-abundant precursors and operated in aqueous electrolytes. CuHCF and NiHCF are desirable stationary energy storage facilities on the grid because of their long cycle life, high rate capability, and high energy efficiency. NiHCF, which has a lower reaction potential than CuHCF for a variety of insertion ions, is more stable than CuHCF during long-term cycling of sodium.[10] Here, the copper−nickel hexacyanoferrate (CuNiHCF) system was examined in an effort to raise the reaction potential of NiHCF, while still retaining its superb stability during sodium ion cycling. Optimization of the CuNiHCF material system will allow development of higher voltage aqueous sodium ion full cells with extremely long cycle life.

Prussian Blue analogues such as CuNiHCF have a face-centered cubic structure in which octahedrally coordinated transition metal hexacyanides form an open framework with 6-fold, nitrogen-coordinated transition metals (Figure 1a).[11] Hydrated alkaline ions or zeolitic water may occupy the interstitial "A Sites" within the framework. Materials with this structure may therefore be represented by $A_xP_y[R(CN)_6]_z \cdot nH_2O$, where A is an alkaline ion and P and R are transition metal ions. During the reversible electrochemical cycling of these materials, alkaline ions are inserted or removed from the A Sites, with a corresponding change in the valence of either the P or R site ion. For example, the electrochemical reduction of iron in CuHCF during K^+ intercalation may be described by: $KCuFe^{(III)}(CN)_6 + xe^- + xK^+ = K_{1+x}Cu[Fe^{(II)}(CN)_6]_x[Fe^{(II)}(CN)_6]_{1-x}$. Changing the electrochemically active species at the P or R sites results in a change in the reaction potential of the material. In this work, the concentrations of electrochemically inert Cu^{2+} or Ni^{2+} on the P Sites were varied to tune the reaction potential of electrochemically active iron on the R sites.

Previous study of the electrochemical properties of Prussian Blue and its analogues focused on the behavior of electrodeposited thin films, which in some cases were shown to have very long cycle life.[12−14] Though the majority of work on these materials examined their electrochromic properties, the development of thin film Prussian Blue analogue batteries was also investigated.[15−19] The thin film electrodes in those studies had thicknesses of less than 300 nm, and mass loading on the order of $\mu m/cm^2$. Recently, we demonstrated successful cycling of bulk Prussian Blue analogue electrodes with high enough mass loading (about 10 mg/cm^2) for practical use.[8−10]

Most investigations of Prussian Blue analogues have examined "pure" materials, in which only one species occupies the A, P, or R sites; however, the framework structure of these materials allows multiple species to occupy each site. This was demonstrated for A, P, and R site ions.[20−23] Precipitated cadmium−iron hexacyanoferrate particles showed complex changes in crystal structure and electrochemical properties as the Cd/Fe ratio varied, and it was shown that Cd and Fe can occupy both the P and A sites.[21] In contrast, simple solid-solution behavior with no abrupt changes in crystal structure was observed for nickel−iron hexacyanoferrate, and copper−nickel hexacyanoferrate−hexacyanocobaltate particles.[20,22]

A recent study of CuHCF and NiHCF found that each of these materials reversibly intercalates ions including Li^+, Na^+, K^+, and NH_4^+.[10] The hexacyanoferrate group is electrochemically active in both materials, but at a higher potential in CuHCF than in NiHCF. The effect of the P site species in pure materials on the reaction potential of the hexacyanoferrate groups was previously examined.[24] In this work, the physical and electrochemical properties of CuNiHCF materials with intermediate compositions were studied. The nanoparticulate morphology of CuNiHCF allows advanced imaging techniques such as scanning transmission electron microscopy (STEM) energy dispersive X-ray spectroscopy (EDS) to be used to directly relate composition to reaction potential. In addition, CuNiHCF is synthesized in bulk at or near room temperature from earth-abundant materials, and operates in low-cost aqueous devices, making it attractive for large-scale energy storage on the grid. The development of electrode materials with tunable potentials will allow optimization of full cell voltages, which is especially important for aqueous cells with limited electrolyte stability.

RESULTS AND DISCUSSION

CuNiHCF materials with a variety of compositions were synthesized by a previously described coprecipitation method.[8−10] The relative concentrations of Cu, Ni, and Fe in these materials were found using inductively coupled plasma mass spectrometry (ICP−MS). Fresh CuNiHCF nanoparticles were used for physical characterization, while slurry electrodes containing CuNiHCF were used for electrochemical measurements.

Transmission electron microscopy (TEM) of CuNiHCF showed that these materials are composed of large agglomerations of 20−50 nm nanoparticles (Figure 1b). Both TEM selected area electron diffraction and powder X-ray diffraction found these phase-pure materials to have the face-centered cubic Prussian Blue crystal structure (Figure 1c, 2a), and TEM EDS confirmed the presence of both Cu and Ni in CuNiHCF (Cu/Ni = 0.56:0.44), but only Cu in CuHCF and Ni in NiHCF (Figure 1d). This latter result

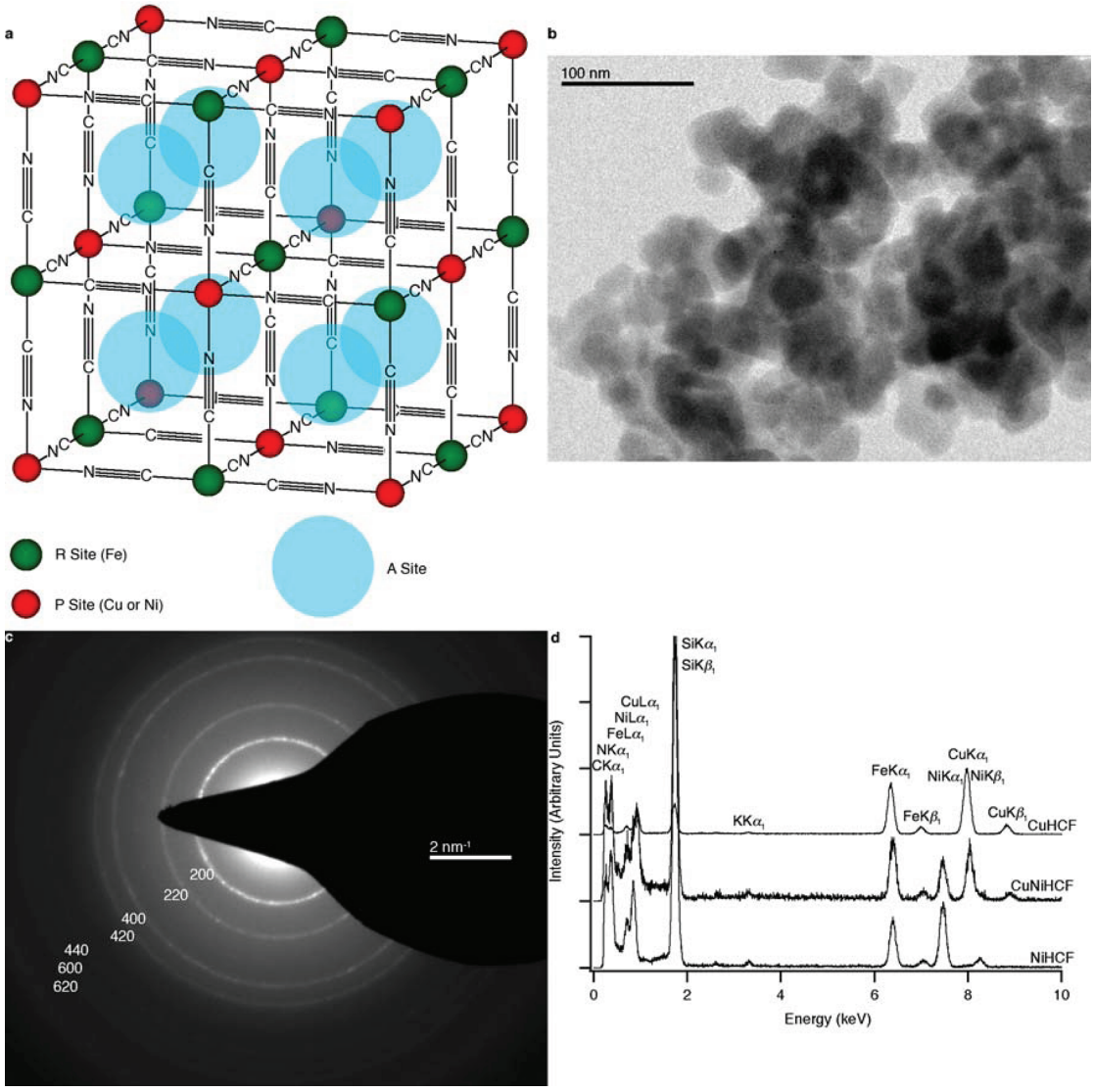

Figure 1. (a) The unit cell of CuNiHCF contains a framework of hexacyanoferrate groups linked by nitrogen coordinated P site transition-metal ions such as Cu and Ni. The large, interstitial A sites may contain either hydrated alkaline ions or zeolitic water. (b) TEM reveals that CuNiHCF is composed of agglomerations of 20−50 nm particles. (c) The TEM electron diffraction pattern of CuNiHCF is consistent with the Prussian Blue crystal structure. (d) TEM EDS shows that CuNiHCF (Cu/Ni = 0.56:0.44) contains both Cu and Ni, while pure CuHCF and NiHCF contain only Cu or Ni, respectively.

corroborates the ICP−MS elemental analysis. The positions of the X-ray diffraction peaks of CuNiHCF were observed to shift to lower angles with increasing Ni content (Figure 2b). This shift corresponds to a roughly linear increase in lattice parameter with increasing Ni content between the lattice parameters of pure CuHCF and NiHCF (Figure 2c). The lattice parameter of Prussian Blue analogues also varies with charge state.[8,9,25] The various CuNiHCF materials had different initial charge states, complicating the effect of composition on the lattice parameter. Nevertheless, the general trend to larger lattice parameters with increasing nickel content is clear.

Previous examinations of mixed hexacyanoferrates have typically used the combination of X-ray diffraction and cyclic voltammetry techniques to assess whether or not multiple species occupy the P sites of the structure.[20−23] For mixed hexacyanoferrates showing more complicated behavior, such as the mixed occupancy of both the P and A sites, sophisticated techniques such as Mossbauer spectroscopy and electron spin resonance have been used to elucidate the structure.[21] To the authors' knowledge, in no instance has the atomic scale homogeneity of a mixed Prussian Blue analogue been directly observed by using an imaging technique such as TEM EDS. Wide-area TEM EDS imaging (Figure 1d) of CuHCF, CuNiHCF (Cu/Ni = 56:44), and NiHCF confirmed the presence of both Cu and Ni in only the CuNiHCF sample, but do not provide information about the homogeneity of CuNiHCF. However, STEM EDS mapping of CuNiHCF nanoparticles conclusively reveals that Cu, Ni, and Fe are distributed throughout each nanoparticle (Figure 3).

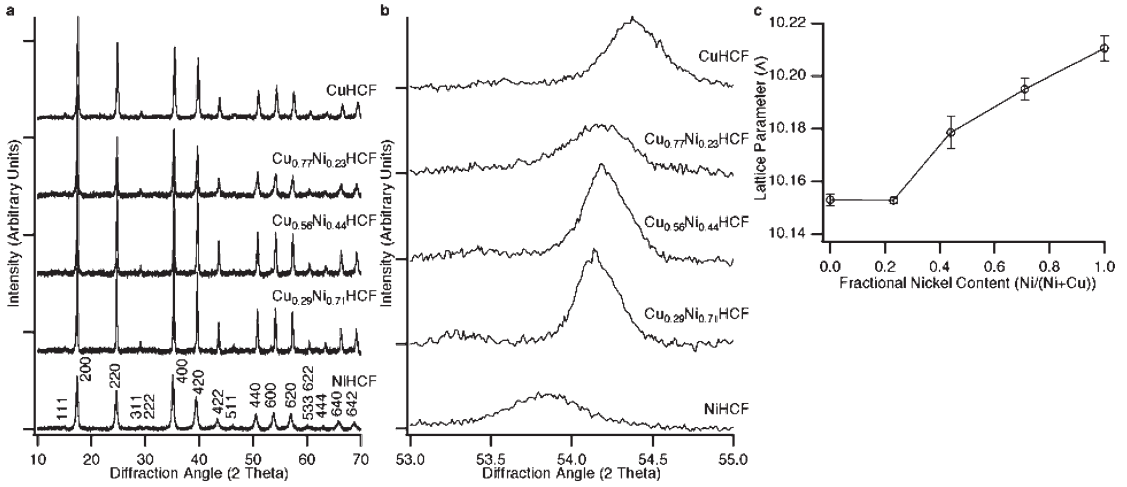

Figure 2. (a) The wide-angle X-ray diffraction spectra of the CuNiHCF powders reveal that the materials are highly crystalline, have the FCC Prussian Blue structure, and contain no impurity phases. (b) A slight peak shift to lower angles is observed as the Ni content of CuNiHCF increases, as illustrated by the shift of the 600 peak. (e) The lattice parameter of CuNiHCF increases with increasing Ni content. This trend is complicated by differences in charge states of the samples.

The distribution of Cu appears to be less homogeneous than those of Ni and Fe; however, this may result from the limited resolution and contrast of the STEM EDS technique. Thus, quantitative conclusions about nanoparticle homogeneity cannot be drawn from the STEM EDS map alone. Nevertheless, it confirms that CuNiHCF is a single phase containing a mixture of Cu and Ni, rather than a mixture of multiple pure phases of CuHCF and NiHCF.

The single-phase nature of CuNiHCF was also studied by electrochemical characterization using aqueous half-cells. Working electrodes and counter-electrodes were prepared as previously described.[8−10] The electrolytes used were 1 M $NaNO_3$ or 1 M KNO_3, with HNO_3 added to lower the pH to 2. Galvanostatic cycling of potassium ions (Figure 4a) and sodium ions (Figure 4b) was performed on CuNiHCF electrodes at ±50 mA/g (about 0.8C). Specific capacities of between 50 and 65 mAh/g, typical for Prussian Blue analogues, were observed during both sodium and potassium ion cycling. The limited control of electrode mass loading on the porous carbon cloth substrates resulted in some variation in the specific capacity of the electrodes. Though these specific capacities are about one-third of those observed for common lithium-ion cathodes, for stationary storage applications a high specific capacity is less important than long cycle life, high power, and high energy efficiency.[1]

At 50 mA/g, CuNiHCF electrodes had voltage hystereses at half-charge of less than 13 mV during potassium ion cycling, and less than 25 mV during sodium ion cycling. These low voltage hystereses indicate the rapid kinetics for alkali ion cycling in CuNiHCF. The low voltage hysteresis of CuNiHCF during cycling will allow full cells using CuNiHCF cathodes to achieve very high round trip energy efficiencies. For example, a hypothetical one-volt cell using a CuNiHCF

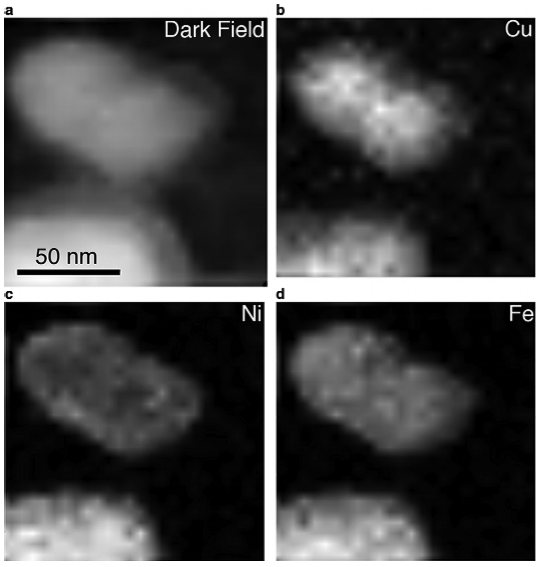

Figure 3. (a) Dark-field scanning TEM of individual $Cu_{0.56}Ni_{0.44}HCF$ nanoparticles. (b,c,d) EDS maps of Cu, Ni, and Fe, respectively, in the same nanoparticles. A homogeneous distribution of these elements is observed.

cathode and a highly reversible anode such as activated carbon can achieve a round trip energy efficiency of over 95% at modest current densities. The rate capabilities of CuHCF and NiHCF electrodes were recently explored in detail.[8−10]

At every tested composition, the reaction potential of CuNiHCF has the "S-curve" shape that is characteristic of a solid solution insertion reaction. Advanced electrochemical characterization such as the galvanostatic intermittent titration technique (GITT) is needed to quantitatively determine the true equilibrium reaction potential of an electrode. However, the extremely low voltage hystereses observed during galvanostatic cycling at 50 mA/g allow ready estimation of the half-charge reaction potentials. The reaction potential of

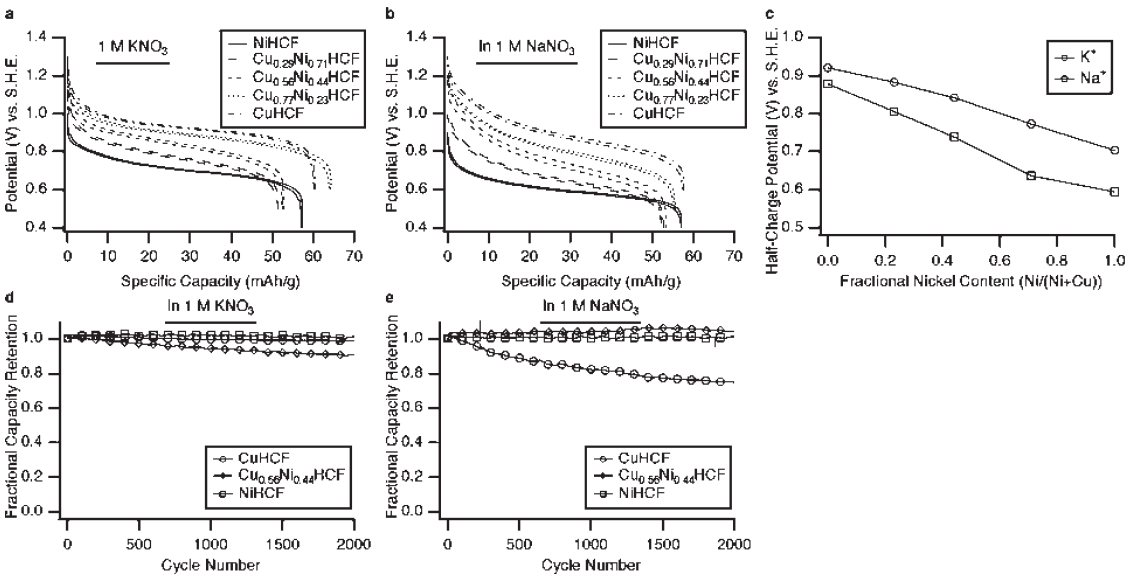

Figure 4. (a) Potential profiles of CuNiHCF during galvanostatic cycling in 1 M KNO_3. (b) Potential profiles of CuNiHCF during galvanostatic cycling in 1 M $NaNO_3$. (c) The reaction potential of CuNiHCF decreases with increasing Ni content in both sodium and potassium electrolytes. CuNiHCF reacts with potassium at higher potentials than it does with sodium. (d) CuHCF and NiHCF show no capacity loss after 2000 cycles at 500 mA/g in 1 M KNO_3, while $Cu_{0.56}Ni_{0.44}HCF$ shows a capacity loss of 9%. (e) NiHCF and $Cu_{0.56}Ni_{0.44}HCF$ show no capacity loss after 2000 cycles at 500 mA/g in 1 M $NaNO_3$, while CuHCF loses 25% of its capacity. NiHCF cycling data were previously reported in ref 9.

CuNiHCF with both potassium and sodium ions decreases dramatically with increasing Ni content (Figure 4c), but the shapes of the potential profiles do not change substantially. The steady change in the reaction potential and lattice parameter with changes in composition, accompanied by a consistent potential profile, provide evidence that Cu and Ni are randomly distributed on the P sites in the CuNiHCF structure. The reaction of CuNiHCF with potassium ions occurs at much higher potentials than its reaction with sodium ions (Figure 4c). For example, the half-charge reaction potential of CuNiHCF (Cu/Ni = 0.56:0.44) with sodium is 144 mV higher than that of NiHCF. This is consistent with prior studies on bulk and thin film Prussian Blue analogues, which found higher reaction potentials for heavier alkali insertion ions.[9,10,26]

The potential of the electrochemically active hexacyanoferrate group has been shown to depend strongly on the nitrogen-coordinated species, and hexacyanoferrates with smaller, more highly charged nitrogen-coordinated transition metals typically have higher reaction potentials.[24] Prior studies found that the reaction potentials of mixed hexacyanoferrates vary smoothly as the fractional occupancy of each species in the P sites in the crystal structure varies.[20,21,23] However, the reaction potentials were found to remain constant when changes in composition were due partial occupancy of the A sites by transition metals, and not changes in the occupancy of the P sites.[21,23] In addition, substantial changes in the occupancy of the A sites by transition metals results in more complicated electrochemical behavior,[23] rather than a single, smooth potential profile. Finally, the roughly linear change in the lattice parameter of CuNiHCF with composition is consistent with the Vegard's law behavior commonly observed for substitutional alloys. Together, electrochemical and X-ray diffraction data provide robust evidence that Cu and Ni form a fully miscible solution on the P sites in the CuNiHCF structure.

The ability to control the reaction potential of CuNiHCF is especially desirable because it operates in aqueous cells, which have a narrow, pH-dependent electrolyte stability window. The reaction potential of CuNiHCF can be tuned to optimize its position with regard to the stability of the electrolyte. Doing so will help allow the use of the entire stability window of the electrolyte, resulting in higher voltage full cells.

Long-term electrochemical cycling of CuHCF, NiHCF, and CuNiHCF (Cu/Ni = 0.56:0.44) was performed in both electrolytes. At 500 mA/g (250 mA/g for CuHCF) in KNO_3, CuHCF and NiHCF show zero capacity loss for 2000 cycles, but CuNiHCF shows a capacity loss of 9% (Figure 4d). CuHCF was found to slowly lose capacity during much longer potassium ion cycling.[8,10] One mechanism for capacity loss is slow dissolution of the electrodes, the rate of which depends on the insertion ion species and pH. The relative concentration of Cu and Ni may also affect the chemical stability of CuNiHCF, but the long-term cycling reported here shows no conclusive trends. NiHCF and CuNiHCF show zero capacity loss for 2000 cycles when cycled at 500 mA/g in 1 M $NaNO_3$, while CuHCF loses 25% of its capacity when cycled under these conditions (Figure 4e). The cycling data for NiHCF was previously reported.[9] Therefore, CuNiHCF can be used in aqueous sodium ion

batteries with higher full cell voltages, while still maintaining the excellent cycle life previously observed for NiHCF.

Prussian Blue analogues such as CuNiHCF are desirable for use as battery electrodes because of their scalable synthesis, operation in inexpensive, safe aqueous electrolytes, long cycle life, and high rate performance and energy efficiency. TEM EDS mapping of CuNiHCF reveals that it is a single, homogeneous phase, with Cu, Ni, and Fe distributed throughout the individual nanoparticles. The consistent changes in lattice parameter and reaction potential, in combination with the smooth potential profiles demonstrate that Cu and Ni form a fully miscible solution on the P sites of the CuNiHCF crystal structure. The reaction potential of CuNiHCF with both sodium and potassium may be easily tuned to a desired value by altering the amounts of Cu and Ni present in the structure. Extremely long cycle life was demonstrated for pure CuHCF and NiHCF samples, as well as an intermediate case, $Cu_{0.56}Ni_{0.44}HCF$. The CuNiHCF material system therefore provides the opportunity to tune the reaction potential without sacrificing other performance characteristics such as cycle life. CuNiHCF cathodes can be used to maximize the full cell voltage of aqueous sodium and potassium ion batteries with the long cycle life, high power, energy efficiency, and low cost necessary for integration with the electrical power grid.

METHODS

Nanoparticulate CuNiHCF was synthesized using a precipitation method, as described previously.[8−10] An aqueous precursor containing desired quantities of $Cu(NO_3)_2$ and $Ni(NO_3)_2$ with a total concentration of 40 mM was combined in pure water with another aqueous precursor containing 20 mM $K_3Fe(CN)_6$ by simultaneous, dropwise addition. CuNiHCF rapidly precipitated. These precipitates were filtered, washed with water, and dried in vacuum at room temperature. The Cu:Ni ratio in the final CuNiHCF precipitates was close to the Cu:Ni ratio in the aqueous precursor. For example, a 50:50 ratio of Cu:Ni in the precursor resulted in a 56:44 ratio of Cu:Ni in the solid product. This slight excess of copper in the final product was observed for all intermediate compositions in the CuNiHCF system. Battery electrodes with mass loadings of approximately 5−10 mg CuNiHCF/cm^2 were prepared as reported previously,[8−10] and studied in three electrode flooded cells that contained excess aqueous electrolyte, CuNiHCF working electrode, a Ag/AgCl reference electrode, and a large, partially charged NiHCF counter-electrode that acted as a reversible ion sink. The electrolytes used were 1 M KNO_3 and 1 M $NaNO_3$, with HNO_3 added to lower the pH to 2.

Conflict of Interest: The authors declare no competing financial interest.

Acknowledgment. The authors acknowledge support from the King Abdullah University of Science and Technology (KAUST) Investigator Award (No. KUS-I1-001-12). They also acknowledge the Department of Energy, Office of Basic Energy Sciences, Division of Materials Sciences and Engineering under contract DE-AC02-76SF00515 through the SLAC National Accelerator Laboratory LDRD project.

REFERENCES AND NOTES

1. Rastler, D. *Electrical Energy Storage Technology Options*; Electric Power Research Institute: Palo Alto, CA, 2010; pp 1−170.
2. LaCommare, K. H.; Eto, J. H. *Understanding the Cost of Power Interruptions to the U.S. Electricity Consumers*; DOE Environmental Energy Technologies Division: Berkeley, CA, 2004; pp 1−70.
3. Yang, Z.; Zhang, J.; Kintner-Meyer, M. C. W.; Lu, X.; Choi, D.; Lemmon, J. P.; Liu, J. Electrochemical Energy Storage for Green Grid. *Chem. Rev.* **2008**, *111*, 3577–3613.
4. Soloveichik, G. L. Battery Technologies for Large-Scale Energy Storage. *Annu. Rev. Chem. Biomol. Eng.* **2011**, *2*, 503–527.
5. Ruffo, R.; Wessells, C.; Huggins, R. A.; Cui, Y. Electrochemical Behavior of $LiCoO_2$ as Aqueous Lithium-Ion Battery Electrodes. *Electrochem. Commun.* **2009**, *11*, 247–249.
6. Luo, J.-Y.; Cui, W.-J.; He, P.; Xia, Y.-Y. Raising the Cycling Stability of Aqueous Lithium-Ion Batteries by Eliminating Oxygen in the Electrolyte. *Nat. Chem.* **2010**, *2*, 760–765.
7. Whitacre, J. F.; Tevar, A.; Sharma, S. $Na_4Mn_9O_{18}$ as a Positive Electrode Material for an Aqueous Electrolyte Sodium-Ion Energy Storage Device. *Electrochem. Commun.* **2010**, *12*, 463–466.
8. Wessells, C. D.; Huggins, R. A.; Cui, Y. Copper Hexacyanoferrate Battery Electrodes with Long Cycle Life and High Power. *Nat. Commun.* **2010**, *2*, 550, 10.1038/ncomms1563.
9. Wessells, C. D.; Peddada, S. V.; Huggins, R. A.; Cui, Y. Nickel Hexacyanoferrate Nanoparticle Electrodes for Aqueous Sodium and Potassium Ion Batteries. *Nano Lett.* **2011**, *11*, 5421–5425.
10. Wessells, C. D.; Peddada, S. V.; McDowell, M. T.; Huggins, R. A.; Cui, Y. The Effect of Insertion Species on Nanostructured Open Framework Hexacyanoferrate Battery Electrodes. *J. Electrochem. Soc.* **2012**, *159*, A98–A103.
11. Buser, H. J.; Schwarzenbach, D.; Petter, W.; Ludi, A. The Crystal Structure of Prussian Blue: $Fe_4[Fe(CN)_6]_3 \cdot xH_2O$. *Inorg. Chem.* **1977**, *16*, 2704–2710.
12. Neff, V. D. Electrochemical Oxidation and Reduction of Thin Films of Prussian Blue. *J. Electrochem. Soc.* **1978**, *125*, 886–887.
13. Oi, T. Electrochromic Materials. *Annu. Rev. Mater., Sci.* **1986**, *16*, 185–201.
14. Stilwell, D. E.; Park, K. H.; Miles, M. H. Electrochemical Studies of the Factors Influencing the Cycle Stability of Prussian Blue Films. *J. Appl. Electrochem.* **1992**, *22*, 325–331.
15. Neff, V. D. Electrochemical Oxidation and Reduction of Thin Films of Prussian Blue. *J. Electrochem. Soc.* **1985**, *132*, 1382–1384.
16. Grabner, E. W.; Kalwellis-Mohn, S. Hexacyanoferrate Layers as Electrodes for Secondary Cells. *J. Appl. Electrochem.* **1986**, *17*, 653–656.
17. Honda, K.; Hayashi, H. Prussian Blue Containing Nafion Composite Film as Rechargeable Battery. *J. Electrochem. Soc.* **1987**, *134*, 1330–1334.
18. Kaneko, M.; Okada, T. A Secondary Battery Composed of Multilayer Prussian Blue and Its Reaction Characteristics. *J. Electroanal. Chem.* **1988**, *255*, 45–52.
19. Kalwellis-Mohn, S.; Grabner, E. W. A Secondary Cell Based on Thin Layers of Zeolite-like Nickel Hexacyanometallates. *Electrochem. Acta* **1989**, *34*, 1265–1269.
20. Reddy, S.; Dostal, A.; Scholz, F. Solid State Electrochemical Studies of Mixed Nickel-Iron Hexacyanoferrates with the Help of Abrasive Stripping Voltammetry. *J. Electroanal. Chem.* **1996**, *403*, 209–212.
21. Zakharchuk, N. F.; Naumov, N.; Stösser, R.; Schröder, U.; Scholz, F.; Mehner, H. Solid State Electrochemistry, X-ray Powder Diffraction, Magnetic Susceptibility, Electron Spin

Resonance, Mossbauer and Diffuse Reflectance Spectroscopy of Mixed Iron(III)−Cadmium(II) Hexacyanoferrates. *J. Solid State Electrochem.* **1999**, *3*, 264–276.
22. Widmann, A.; Kahlert, H.; Petrovic-Prelevic, I.; Wulff, H.; Yakhmi, J. V.; Baghar, N.; Scholz, F. Structure, Insertion Electrochemistry, and Magnetic Properties of a New Type of Substitutional Solid Solutions of Copper, Nickel, and Iron Hexacyanoferrates/Hexacyanocobaltates. *Inorg. Chem.* **2002**, *41*, 5706–5715.
23. Kulesza, P. J.; Malik, M. A.; Schmidt, R.; Smolinska, A.; Miecznikowski, K.; Zamponi, S.; Czerwinski, A.; Berrettoni, M.; Marassi, R. Electrochemical Preparation and Characterization of Electrodes Modified with Mixed Hexacyanoferrates of Nickel and Palladium. *J. Electroanal. Chem.* **2000**, *487*, 57–65.
24. Scholz, F.; Dostal, A. The Formal Potentials of Solid Metal Hexacyanoferrates. *Angew. Chem., Int. Ed. Engl.* **1995**, *34*, 2685–2687.
25. Dostal, A.; Kauschka, G.; Reddy, S.; Scholz, F. Lattice Contractions and Expansions Accompanying the Electrochemical Conversions of Prussian Blue and the Reversible and Irreversible Insertion of Rubidium and Thallium Ions. *J. Electroanal. Chem.* **1996**, *406*, 155–163.
26. McCargar, J. W.; Neff, V. D. Thermodynamics of Mixed-Valence Intercalation Reactions: The Electrochemical Reduction of Prussian Blue. *J. Phys. Chem.* **1988**, *92*, 3598–3604.